J Mater Sci (2018) 53:4814–4827

Ceramics

Improved methods for nanoindentation Berkovich probe calibrations using fused silica

Joseph E. Jakes[1,*]

[1] *Forest Biopolymers Science and Engineering, USDA Forest Service, Forest Products Laboratory, One Gifford Pinchot Drive, Madison, WI 53726, USA*

Received: 6 October 2017
Accepted: 12 December 2017
Published online: 20 December 2017

ABSTRACT

Improved methods are needed to improve the reliability and reporting of Berkovich probe calibrations. Current methods for calibrating machine compliance rely substantially on the subjectivity of the user to choose and exclude from the analysis nanoindentations below a threshold size that are affected by probe tip imperfections or the fused silica surface properties. Furthermore, it can be difficult to identify erroneous experimental data, such as those resulting from dirty or damaged probes. To help overcome these issues in Berkovich probe calibrations, a pre-nanoindentation liftoff analysis and systematic analysis of the Stone–Yoder–Sproul plot were developed. The utility of the analyses was demonstrated through analysis of experimental data. After correcting the fused silica data for machine compliance, the probe area function calibration was performed following established protocols. Finally, a concise protocol for reporting Berkovich probe calibration results was established to improve comparisons between experiments performed with different Berkovich probes.

Introduction

In nanoindentation, a carefully shaped probe is pressed into a material, while the applied load and depth of penetration are continuously monitored. Then, from the resulting load–depth trace and a probe area function, the material mechanical properties, most often elastic modulus and hardness, are calculated [1, 2]. An advantage of nanoindentation over other mechanical testing techniques is its ability to probe small volumes of materials [3–5]. By utilizing the probe area function, the contact area can be calculated without having to laboriously measure the contact area from images of residual indentation impressions, such as typically done in conventional hardness testing [3–5]. However, two important factors that are critical to the accuracy of the nanoindentation results are machine compliance and probe area function calibrations [1, 6]. Many potential issues can affect the accuracy of these calibrations, including a dirty or damaged probe, calibration material surface properties, operator bias, and errors in data fitting, and these issues often affect the calibrations unbeknownst to the operator. This is a problem because the effects of these issues can substantially

Address correspondence to E-mail: jjakes@fs.fed.us

https://doi.org/10.1007/s10853-017-1922-8

affect the accuracy of the calibrations and subsequent experimental results obtained using the calibrations.

During nanoindentation, the displacement measured by the instrument includes both the depth of penetration into the material surface and the displacement from the deflection of the instrument during loading. This instrument deflection must be calculated and subtracted from the measured displacement to accurately assess the depth of penetration. Nanoindenters are typically designed so the instrument deflection depends linearly on load. This deflection is quantified using a constant called the machine compliance, which is defined as the instrument deflection divided by applied load. Using machine compliance, displacement arising from the instrument deflection at a given load is calculated and subtracted from measured displacement to determine penetration depth. However, directly measuring instrument deflection to calculate machine compliance is difficult for an operator. Therefore, machine compliance is typically determined using results from nanoindentation experiments in a calibration material with known properties [1, 4, 5, 7].

For the common three-sided pyramidal Berkovich probe [8], the machine compliance is often determined using a series of quasistatic nanoindentations or a continuous stiffness nanoindentation in a fused silica calibration standard. This same set of calibration data is also used to calculate the probe area function. Fused silica is considered an acceptable calibration material because it is assumed to be a homogeneous material with known elastic modulus and hardness. An ideal Berkovich probe is geometrically self-similar, which means when testing a homogeneous material such as fused silica the assessed mechanical properties can be assumed to be independent of nanoindentation size. Many of the commonly used analyses for machine compliance calibration rely on this assumption [1, 6, 7]. However, in practice, this assumption is violated at low loads because of tip imperfections and fused silica surface properties. Tip imperfections refer to any deviation of the Berkovich probe from its ideal shape near its tip, which may include rounding, flattening, or some other irregularity. It is well known that for real Berkovich probes, the geometrically self-similar assumption is violated below a threshold nanoindentation size, and measured properties, especially hardness, have an indentation size effect caused by tip imperfections [1, 9–12]. This geometric indentation size effect is different than the intrinsic material size effects often studied using nanoindentation [13]. Fused silica surfaces also have roughness and modified surface chemical properties that can result in inhomogeneous surface mechanical properties. Additionally, at high loads, cracking may occur during the experiment. Therefore, a user must identify and exclude nanoindentations affected by probe tip imperfections, fused silica surface effects, and cracking in order to meet the assumption of size-independent mechanical properties in the calculation of machine compliance. Cracking can typically be identified by a pop-in on the load–depth trace or by microscopy of the residual nanoindentation impression. Unfortunately, the choice for the threshold nanoindentation size below which the data are affected by tip imperfections and surface properties is subjective, and the machine compliance and subsequent probe area function can be substantially affected by user bias.

The size of the tip imperfections will vary between Berkovich probes, and the utility of a probe for a given application is often dictated by the size of the probe's tip imperfections. For example, when testing thin films, small tip imperfections are desired because the fully formed Berkovich plastic zone can be developed at smaller nanoindentation sizes, which can reduce substrate effects [10]. Similarly, when using the structural compliance method to remove edge effects on a material like wood cell walls, it is necessary to use only the range of nanoindentation sizes over which elastic modulus and hardness are independent of nanoindentation size and not affected by tip imperfections [14–16]. Minimal tip imperfections are also desired in the deconvolution of geometric indentation size effects caused by tip imperfections, and the intrinsic material indentation size effects that are often of interest in nanoindentation studies [13]. Tip imperfections in Berkovich probes are commonly conceptualized by assuming the tip of the probe is spherical, and estimates of the radius of the spherical tip are used as a metric of the probe quality. The tip radius can be estimated directly using a scanning probe microscopy image of the tip or indirectly using the truncation depth estimated from a series of calibration nanoindentations [11]. However, in practice, whether a Berkovich probe tip is spherical, flat, or exhibits some other geometric irregularity is inconsequential. The essential parameter is the threshold nanoindentation size

above which tip imperfections are overcome and the experimental results are characteristic of a Berkovich geometrically self-similar probe.

A dirty probe is another potential issue that can adversely affect fused silica calibration nanoindentations. Debris attached to the surface of a dirty probe can affect the detection of initial contact between the probe and fused silica surface, or the mechanical response during the nanoindentation experiment. The most direct way to determine whether or not a probe is clean is to look at a high-resolution image of the probe. However, imaging a probe is not always practical. Also, it is possible for the probe to pick up debris from the fused silica surface during a series of nanoindentations. Although observing that a probe is dirty is sometimes obvious in nanoindentation data, it can also be difficult because the effects can be subtle. Performing machine compliance and probe area function calibrations using data affected by a dirty probe will result in incorrect calibrations.

In this paper, improved methods are developed for Berkovich probe fused silica calibrations. First, an analysis of the pre-nanoindentation liftoff load–depth trace is demonstrated to check for a dirty probe with debris protruding from its tip and to define the initial point of contact between the probe tip and fused silica surface. Then, the area-independent Stone–Yoder–Sproul (SYS) correlation [7] is utilized to directly determine the machine compliance. A systematic SYS plot analysis is developed to minimize user subjectivity in identifying the smaller nanoindentations affected by probe tip imperfections or fused silica surface effects that must be excluded when calculating the machine compliance. The systematic SYS plot analysis is also shown to be useful to detect dirty probes and as a metric of the quality of the fused silica calibrations and probe tip imperfections. Finally, a concise protocol based on the fused silica Berkovich probe calibration results is proposed to report the quality of the probe and fused silica calibrations. This reported information is needed to better facilitate comparisons of nanoindentation results obtained from different Berkovich probes.

Background theory

In nanoindentation, the Meyer hardness (H) is defined as

$$H = \frac{P_0}{A_0} \tag{1}$$

where P_0 and A_0 are the maximum load and contact area, respectively, immediately prior to unloading. In a load–depth (P–h) trace that has been corrected for machine compliance (C_m), the inverse of the initial unloading slope is the contact compliance (C_p), which is the compliance attributable to the specimen and indenter probe. The C_p is related to the "effective" modulus of contact (E_{eff}) through

$$C_p = \frac{1}{E_{eff}A_0^{1/2}} \tag{2}$$

For indentation against a homogenous, isotropic, elastic half-space,

$$\frac{1}{E_{eff}} = \frac{1}{\beta}\frac{\pi^{1/2}}{2}\left(\frac{1-\nu_s^2}{E_s} + \frac{1-\nu_d^2}{E_d}\right) \tag{3}$$

where E_s and E_d are Young's moduli and ν_s and ν_d are Poisson's ratios of specimen and indenter, respectively. β is a numerical factor that is close to 1 [14, 17–19]. For most of the analyses in this paper, $\beta = 1$ is assumed. The effect of β on the probe area function and fused silica H and E_s will be discussed.

Numerous methods are used to estimate C_m. Some of the originally proposed methods rely on measuring A_0 and require either independent measurement of residual contact areas, such as in the Doerner-Nix plot [4], or iterative calculations between C_m and probe area function calibrations, such as originally proposed by Oliver and Pharr in 1992 [5]. Area-independent methods can be the most convenient to directly estimate C_m [1, 6, 7]. In these methods, C_p is assessed as a function of load in a rigidly supported calibration material using either a series of quasistatic nanoindentations or a continuous stiffness nanoindentation. A key requirement of the calibration material is that the elastic modulus and hardness are independent of nanoindentation size. Then, the data from nanoindentations that exhibit size-independent properties are chosen and fit to a function to estimate C_m. In this paper, the Stone–Yoder–Sproul (SYS) [7] correlation is used to estimate C_m and is given by

$$C_t P_0^{1/2} = C_m P_0^{1/2} + J_0^{1/2} \tag{4}$$

where C_t is taken from the inverse of the initial unloading slope from a P–h trace that has not been corrected for C_m, and $J_0^{1/2} = C_p P_0^{1/2} = H^{1/2}/E_{eff}$ is the square root of the Joslin-Oliver parameter [20]. The

material parameter $J_0^{1/2}$ is independent of A_0 and β. If both H and E_{eff} are independent of nanoindentation size, then $J_0^{1/2}$ is also independent of P_0. For Berkovich nanoindentations on fused silica larger than those affected by tip imperfections or fused silica surface properties, $J_0^{1/2}$ is assumed to be independent of P_0, and $C_t P_0^{1/2}$ plotted as a function of $P_0^{1/2}$ forms a straight line of slope C_m and y-intercept of $J_0^{1/2}$.

After correcting the fused silica calibration nanoindentation P–h traces for C_m, the Oliver–Pharr method to calculate a probe area function can then be utilized [1, 5]. The Oliver–Pharr contact depth h_c [5] is calculated for a Berkovich probe using

$$h_c = h_0 - \varepsilon C_p P_0 \tag{5}$$

where h_0 is the depth immediately prior to unloading, and ε is a constant that depends on the probe geometry. Based on results of Sneddon, ε can be determined to be 0.72, 0.75, and 1 for conical, paraboloid of revolution, and punch probe geometries, respectively [21]. Although of these probe geometries a Berkovich probe is most similar to a cone, the paraboloid of revolution value of $\varepsilon = 0.75$ is found to be more appropriate based on experimental observations [5] and finite element analysis [22]. Therefore, $\varepsilon = 0.75$ is used here.

Using the known material and probe elastic properties and combining Eqs. 2 and 3, the calculated area A_0^{calc} is determined for each calibration nanoindentation using

$$A_0^{\text{calc}} = \frac{1}{\beta^2}\frac{1}{C_p^2}\left[\frac{\pi^{1/2}}{2}\left(\frac{1-\nu_s^2}{E_s}+\frac{1-\nu_d^2}{E_d}\right)\right] \tag{6}$$

The probe area function is then calculated by fitting the A_0^{calc}–h_c data from the series of nanoindentations to a function, such as

$$A_0(h_c) = c_0 h_c^2 + \sum_{i=1}^{5} c_i h_c^{1/2^{i-1}} \tag{7}$$

where c_i are fitting parameters. The c_0 can either be a fitting parameter or be set the ideal value of 24.5 for an ideal Berkovich probe. Here, the ideal $c_0 = 24.5$ value is used.

Experimental procedure

A Hysitron (Minneapolis, Minnesota, USA) TI 900 TriboIndenter upgraded with a performech controller was used with two different Berkovich probes. Experiments were performed on the fused silica calibration standard provided by Hysitron. The fused silica was stored in ambient conditions and cleaned before experiments by gently wiping the surface with dry tissue paper. For Probe #1, two sets of data were collected. The first set of Probe #1 data was from when the probe was clean, and this set of data was used to demonstrate acceptable fused silica calibrations. The second set of Probe #1 data was from when the probe was dirty. The probe became dirty while performing experiments on a research material, and the series of fused silica nanoindentations was originally performed to diagnose suspect experimental results. However, the data was used to demonstrate how the proposed analyses can be used to detect a dirty probe. Probe #2 was found to have much larger tip imperfections than Probe #1, and the Probe #2 data were included to show how the proposed analyses can be used to determine probe quality.

The sets of experiments consisted of series of 80-120 load-control quasistatic nanoindentations with P_0 ranging from 0.01 to 12 mN. A 2-μN preload was used, and each nanoindentation was preceded by a pre-nanoindentation liftoff that consisted of a 2-s segment during which the probe was lifted 20 nm and disengaged from the surface, followed by a 2-s reapproach segment. As will be shown in the Results section, an analysis of the pre-nanoindentation liftoff was used to define the initial surface contact and as a check for probe tip cleanliness. The load function consisted of a 5-s load, 5-s hold at P_0, 2-s unload to 40% P_0, 60-s thermal drift segment at 40% P_0, and finally a 1-s unload. The thermal drift was measured from the final 40 s of the thermal drift segment and used to correct the depth of penetration h. The initial unloading stiffness dP/dh at P_0 of each unloading segment was assessed by fitting the Oliver–Pharr power law function $P = A(h - h_f)^m$, where A, h_f, and m are fitting parameters [5], to 40–95% of P_0 in the unloading segment. The E_s of fused silica was calculated using Eqs. 2 and 3, where E_d and ν_d for the diamond probe were assumed to be 1137 GPa and 0.07, respectively, and ν_s for fused silica was assumed to be 0.17. For the calculation of the area function using Eq. 6, $E_s = 72$ GPa was assumed for the fused silica calibration standard.

A Quesant (Agoura Hills, California, USA) atomic force microscope (AFM) incorporated in the TriboIndenter was used to image the Berkovich probe tips and residual nanoindentation impressions in the

fused silica surface. The AFM was operated in contact mode and calibrated in the lateral directions using an Advanced Surface Microscopy (Indianapolis, Indiana, USA) calibration standard as described previously [14]. The AFM depth was calibrated using 19.6-, 113-, and 495-nm step height calibration standards from Budget Sensors (Sofia, Bulgaria).

Results

Pre-nanoindentation liftoff analysis

Debris on a dirty nanoindentation probe may or may not protrude from the probe tip (Fig. 1). An analysis of the pre-nanoindentation liftoff was useful to help detect whether the nanoindentation probe had debris protruding from its tip. Additionally, the zero P and h for the nanoindentations could be defined during this analysis. Figure 2a shows the characteristic P–h trace from the pre-nanoindentation liftoff and approach segments of a probe without debris protruding from its tip. Point 1 in Fig. 2a was the initial P and h at the 2-μN preload immediately preceding the nanoindentation. At the beginning of the pre-nanoindentation liftoff, the 2-μN preload was unloaded, and the probe tip came off the fused silica surface (point 2). Then, the probe was lifted to approximately 20 nm off the surface (point 3) before being moved back toward the surface. At point 4, the initial contact to the surface can be identified by the increase in P, and this point was used to define $h = 0$. An important feature of good liftoff and approach segments was that the P did not systematically vary with h between the liftoff (point 2) and initial contact (point 4). The relatively constant P while the probe was out of contact with the surface was a good indication that no debris was protruding from the probe tip and was also used to define $P = 0$. The slight difference in h between the initial h at preload (point 1) and h following the approach segment was likely a small anelastic rebound. In defining $h = 0$ at point 4, it was assumed that any additional residual depth that may have resulted from plastic deformation caused by the 2-μN preload or initial approach was negligible.

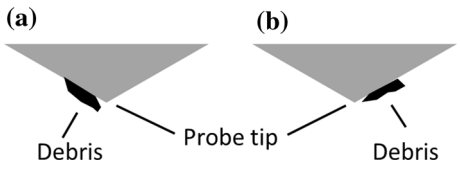

Figure 1 Illustrations showing debris adhered to a probe surface that **a** does and **b** does not protrude beyond the probe tip.

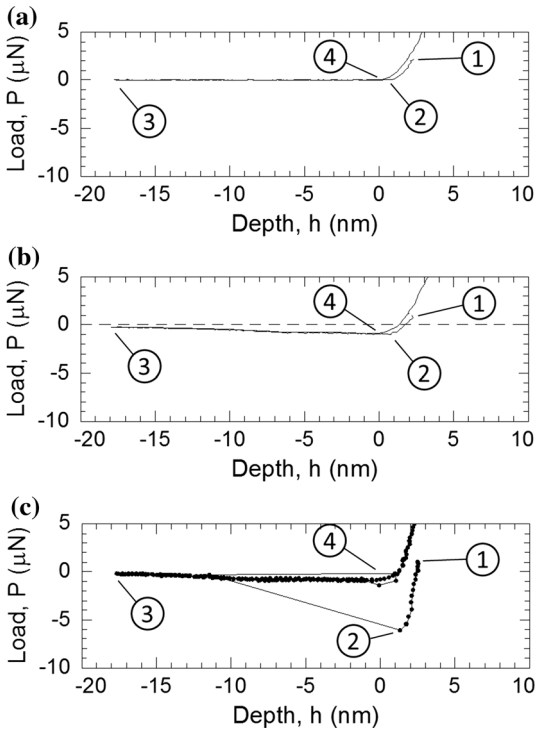

Figure 2 Load–depth (P–h) traces during the pre-nanoindentation liftoff and approach segments from experiments using **a** a clean probe and **b**, **c** dirty probes that likely have debris protruding beyond the probe tip.

Figure 2b and c display P–h traces of liftoff and approach segments indicative of probe tips with protruding debris. In Fig. 2b, the effect was subtle. The only difference between the P–h traces in Fig. 2a and b was that the P between the liftoff (point 2) and initial contact (point 4) in Fig. 2b systematically varied with h and increased the farther the probe was lifted from the surface. This variation in P with h suggested that compliant debris may have been protruding from the tip that bridged between the probe tip and fused silica surface. To make this subtle diagnosis, the transducer spring force calibration and thermal drift correction must also be correct because an incorrect spring force calibration or thermal drift correction would cause a similar variation in P with h. Figure 2c shows another example of a dirty probe. During the liftoff after the initial 2-μN preload (point 1), P became negative, likely because there was debris that caused the probe tip to adhere to the fused silica

surface. At point 2, the probe was released and snapped away from the surface. Observing *P*–*h* traces like those in Fig. 2b and c indicates that the data must not be used for calibrations. In both instances, the probes were cleaned after the experiments using a styrofoam wedge and distilled water under a dissecting microscope. Then, the fused silica calibration nanoindentations were repeated. The repeated nanoindentations liftoff and approach *P*–*h* traces (data not shown) looked like those in Fig. 2a, which further verified that the behavior in Fig. 2b and c was likely caused by debris attached to and protruding from the probe tips.

Figure 2b and c show only two examples of how pre-nanoindentation *P*–*h* traces might behave for a dirty probe with debris protruding from its tip. Other types of behavior may also be observed. Therefore, a good first check of probe cleanliness for all calibration nanoindentations is not that the pre-nanoindentation liftoff and approach segments do not look like the *P*–*h* trace in Fig. 2b and c, but rather that they look similar to Fig. 2a. However, observing the expected pre-nanoindentation *P*–*h* trace is not sufficient to assure a clean probe. Protruding debris may possibly cause a false surface contact that happens to result in a *P*–*h* trace during the pre-nanoindentation liftoff segments that looks like Fig. 2a, or debris may be stuck to the probe that does not protrude from the tip (Fig. 1b) and would therefore not affect the pre-nanoindentation liftoff *P*–*h* trace. In the next section, it will be shown how a systematic SYS plot analysis can also be used to detect dirty probes even if they have the expected pre-nanoindentation liftoff *P*–*h* trace.

Systematic SYS plot analysis

According to the SYS correlation in Eq. 4, the slope of a straightline fit to data in the SYS plot is C_m and the *y*-intercept is $J_0^{1/2}$. Figure 3 shows SYS plots from three sets of fused silica calibration data. Obviously, the entire range of data in the SYS plots did not form a straight line, especially at lower loads where $C_t P_0^{1/2}$ became substantially lower and noisier. The unavoidable effects of probe tip imperfections or fused silica surface properties likely affected the measured mechanical properties at these lower loads, which resulted in a violation of the SYS correlation assumption that H and E_s are independent of load. A fracture event, such as cracking, during a fused silica

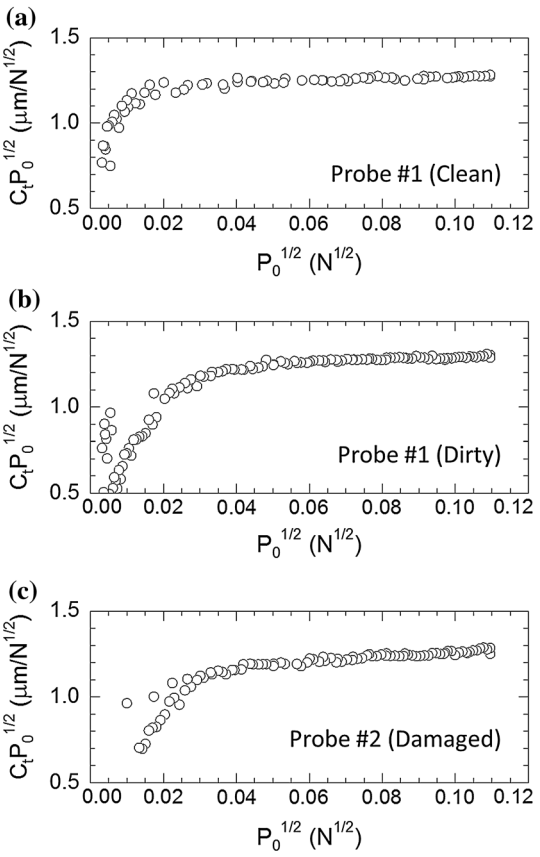

Figure 3 SYS plots from series of Berkovich probe fused silica calibration nanoindentations using **a** Probe #1 when it was clean, **b** Probe #1 when it was dirty, and **c** Probe #2, which was damaged. All the data in these SYS plots had pre-nanoindentation liftoff and approach *P*–*h* traces similar to the trace in Fig. 2a, which indicated that there was not any debris protruding from the probe tip.

nanoindentation would have also caused a violation of this load-independent assumption, and those nanoindentations would have needed to be excluded. For the data presented in this paper, no fracture events were observed in the any of the fused silica *P*–*h* traces, as would have been evidenced by sudden jumps, or "pop-ins," in *P*–*h* traces. Additionally, no cracking was expected for a Berkovich probe over the range of P_0 employed in this study [23]. Therefore, accurate calculation of C_m using the SYS correlation here required only that the affected low-load nanoindentations be identified and excluded from the straightline fit. One current method to identify the affected low-load nanoindentations is to visually choose the range of data that looks like a straight line and fit that subset. Then, the value of the SYS plot $J_0^{1/2}$ can be compared to the expected value of

$J_0^{1/2} = 1.22\ \mu m/N^{1/2}$ for Berkovich probe nanoindentations on fused silica [1, 14] to decide whether or not the calibration data are acceptable. A problem with this method is that visually choosing a range of data that looks like a straight line is subjective. For damaged or dirty probes, it may also be possible to inadvertently choose a range of data that just happens by chance to result in the expected value of SYS plot $J_0^{1/2} = 1.22\ \mu m/N^{1/2}$.

A new analysis was needed to aid in identifying the low-load nanoindentations to exclude in the determination of C_m and detecting dirty or damaged Berkovich probes. The systematic SYS plot analysis was developed for these reasons. The analysis was based on the idea that for data not affected by fracture events, a threshold nanoindentation size exists above which the effects of tip imperfections and fused silica surface properties become negligible on the assessed mechanical properties. Therefore, data from nanoindentations larger than this threshold size in the SYS plot form a straight line because $J_0^{1/2} = H^{1/2}/E_{eff}$ will be a constant. Experimentally, the threshold nanoindentation size and the straightness of the SYS plot above this threshold size were determined by systematically increasing the minimum $P_0^{1/2}$ used for the straightline fit in the SYS plot datum by datum. Then, the resulting C_m and SYS plot $J_0^{1/2}$ are plotted as a function of the minimum SYS plot $P_0^{1/2}$. If a threshold nanoindentation size exists above which the SYS plot is a straight line, then in the systematic SYS plot analysis there will be a minimum SYS plot $P_0^{1/2}$ above which both C_m and $J_0^{1/2}$ are constant values. The systematic SYS plot analyses are shown in Fig. 4 for the SYS plots in Fig. 3. When the minimum SYS plot $P_0^{1/2}$ included the smallest nanoindents, the slope of the straightline fit was higher and the y-intercept was smaller, which results in larger values of C_m and smaller values of $J_0^{1/2}$, respectively. As the minimum SYS plot $P_0^{1/2}$ increased and fewer of the affected lower load nanoindentations were included in the fits, C_m decreased and $J_0^{1/2}$ increased.

In the clean Berkovich Probe #1 systematic SYS plot analysis (Fig. 4a), a threshold nanoindentation size was evident at a minimum SYS plot $P_0^{1/2}$ of about $0.025\ N^{1/2}$. Above this threshold, both C_m and SYS plot $J_0^{1/2}$ were fairly constant values. Above a minimum SYS plot $P_0^{1/2}$ value of about $0.065\ N^{1/2}$, the variability in the C_m and SYS plot $J_0^{1/2}$ values increased because fewer data points were being used

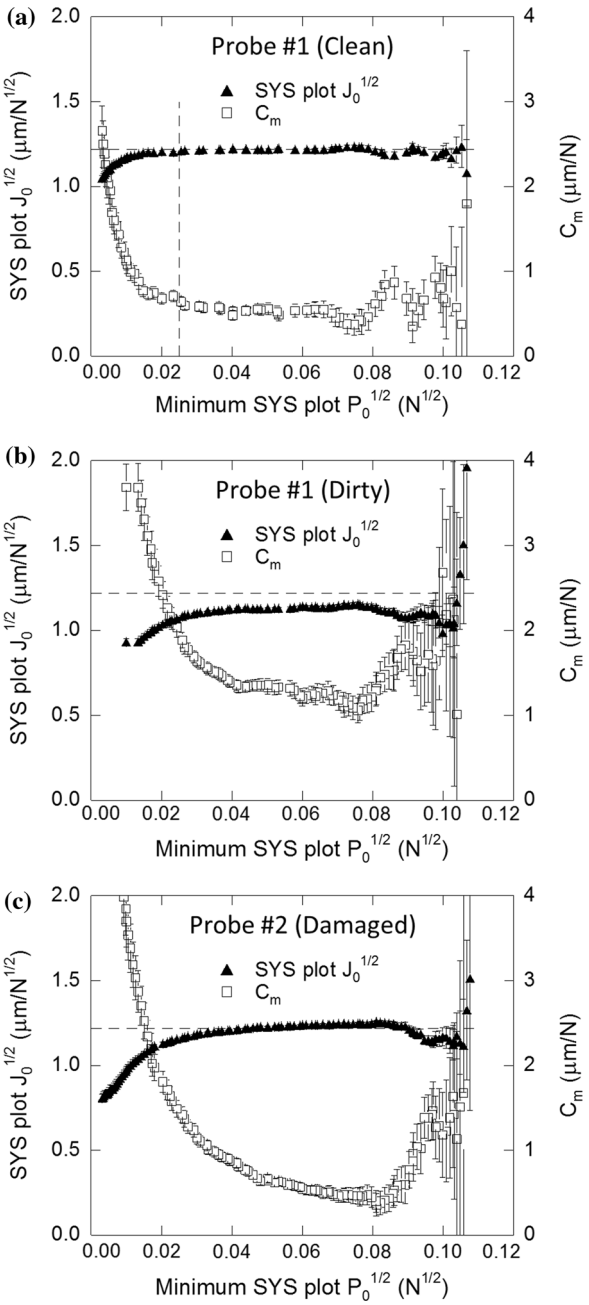

Figure 4 Systematic SYS plot analyses from series of fused silica calibration nanoindentations using **a** Probe #1 when it was clean, **b** Probe #1 when it was dirty, and **c** Probe #2, which was damaged. The SYS plot square root Joslin-Oliver parameters ($J_0^{1/2}$) and machine compliances (C_m) were calculated using the corresponding SYS plots in Fig. 3 and the SYS correlation (Eq. 4) by systematically removing the smallest nanoindentations and fitting a straight line. The horizontal dashed line represents the expected $J_0^{1/2} = 1.22\ \mu m/N^{1/2}$ for Berkovich probe nanoindentations on fused silica [1, 14]. The vertical dashed line in **a** corresponds to the threshold minimum SYS plot $P_0^{1/2} = 0.025\ N^{1/2}$ identified for this data as described in the text. The error bars represent uncertainties based on a least squares analysis for corresponding straightline fits.

in the fits. A further quality check of the calibration was done at this point by comparing the value of SYS plot $J_0^{1/2}$ to the expected value of 1.22 μm/N$^{1/2}$ for Berkovich probe nanoindentations on fused silica [1, 14]. The $J_0^{1/2}$ value for the clean Berkovich Probe #1 was very close to this expected value (Fig. 4a) above the threshold size. Therefore, it was determined that these fused silica calibration data were acceptable and could be used to determine the C_m and probe area function.

The systematic SYS plot analysis was also useful as a sensitive tool to detect dirty and damaged Berkovich probes. Figure 4b shows the systematic SYS plot analysis of the SYS plot in Fig. 3b. It would appear that above a minimum SYS plot $P_0^{1/2}$ value of 0.04 N$^{1/2}$, there were nearly constant values of C_m and $J_0^{1/2}$. However, the average value of $J_0^{1/2}$ was about 1.13 μm/N$^{1/2}$, which was much lower than the expected value of 1.22 μm/N$^{1/2}$. Additionally, the value for C_m was about 1.3 μm/N, which was much higher than the value anticipated based on prior experience with this probe and transducer. These observations led to the conclusion that the probe was either dirty or had become damaged. Visual inspection under a dissecting microscope revealed debris near the probe tip, suggesting the probe was just dirty. This was confirmed after cleaning the probe and the repeated fused silica calibration experiments resulted in an acceptable systematic SYS plot analysis similar to that in Fig. 3a (data not shown).

The systematic SYS plot analysis in Fig. 4c is of the data in Fig. 3c and demonstrates how the analysis can be used to detect a damaged probe. Although $J_0^{1/2}$ was near the expected 1.22 μm/N$^{1/2}$ value for minimum SYS plot $P_0^{1/2}$ between 0.04 and 0.08 N$^{1/2}$, neither C_m nor $J_0^{1/2}$ reached a constant value in this region. In this region, the SYS plot $J_0^{1/2}$ and C_m systematically increased and decreased, respectively. This was suspicious behavior that did not change in repeated calibration experiments even after cleaning the probe. To further investigate the probe cleanliness and tip imperfections, an AFM height image of Probe #2 was obtained (Fig. 5b). For comparison, an image was also obtained of Probe #1 (Fig. 5a). Probe #1 had the anticipated pyramidal shape (Fig. 5a), and in the contour map, a triangular shape could be observed at depths as shallow as 20 nm (Fig. 5c). In contrast, Probe #2 had numerous irregularities near its tip (Fig. 5b). These irregularities manifested as irregular shapes in the contour plots at depths up to 200 nm (Fig. 5d), which covered nearly the entire range of depth in the fused silica calibration experiments. It was therefore decided that Probe #2 had too large of tip imperfections and could not be properly calibrated over the range of nanoindentation sizes obtained in these calibration experiments. The probe may be useful for larger nanoindentations above which the tip imperfections may become negligible.

The necessity of the systematic SYS plot analysis was clearly demonstrated in the analysis of the data from Probe #2. The previous method commonly used to calculate C_m from the SYS plot is to visually choose the range of data that looks like a straight line, fit the data to a straight line, and compare the value of the SYS plot $J_0^{1/2}$ to the expected value of $J_0^{1/2} = 1.22$ μm/N$^{1/2}$. In the SYS plot (Fig. 3c), the data above $P_0^{1/2} = 0.06$ N$^{1/2}$ looked like a straight line. When those data were fitted to a straight line, the value of SYS plot $J_0^{1/2}$ was very near the expected 1.22 μm/N$^{1/2}$ value as seen in the systematic SYS plot analysis (Fig. 4c). This previous analysis would have erroneously led the user to conclude that above $P_0^{1/2} = 0.06$ N$^{1/2}$, the effects of probe tip imperfections and fused silica surface properties became negligible and the probe was behaving like a characteristic Berkovich probe. Only after the systematic SYS plot analysis, it was observed that the probe was not actually behaving like a Berkovich probe. This observation led to further investigation using AFM imaging and the conclusion that the probe tip imperfections for Probe #2 were so large that the probe must be considered damaged and not reliable as a Berkovich probe over this range of nanoindentations sizes.

Fused silica calibration

After determining a set of Berkovich probe fused silica calibration data is acceptable, the C_m and probe area function calibration procedures can proceed as demonstrated here using the clean Probe #1 data (Figs. 3a and 4a). In the systematic SYS plot analysis (Fig. 3a), C_m was observed to vary some even above the threshold minimum SYS plot $P_0^{1/2}$ value of 0.025 N$^{1/2}$. Looking at the reasonable range of values above the threshold nanoindentation size and below the values where the fit uncertainties started to noticeably increase (between 0.025 and 0.065 N$^{1/2}$), the calculated value of C_m ranged between 0.48 and 0.64 μm/N. The average value of $C_m = 0.55$ μm/N was chosen. Although there was an uncertainty on the order of 10% in C_m, this uncertainty had little effect on the A_0^{calc} and h_c used in the probe area

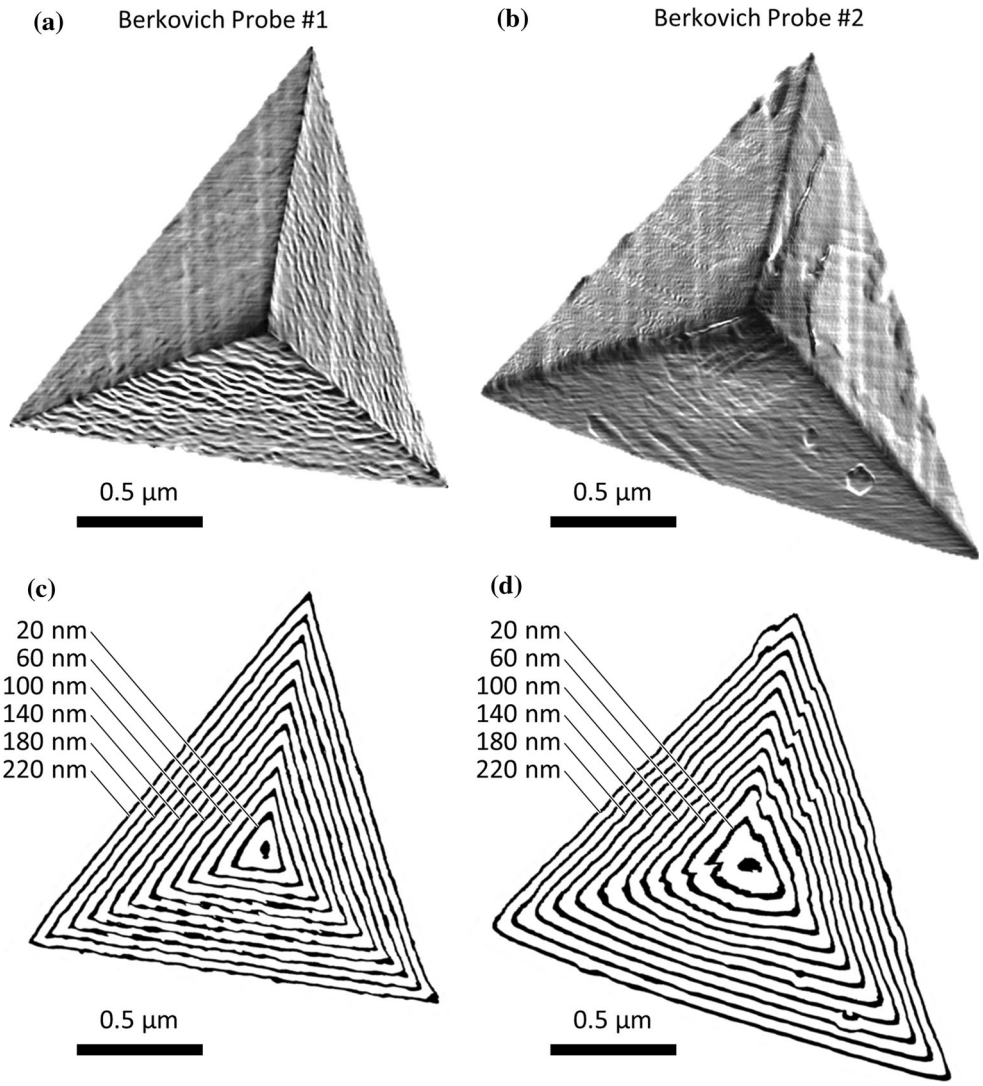

Figure 5 Atomic force microscopy (AFM) height images of **a** Probe #1 and **b** Probe #2. Contour maps are shown in **c** and **d** for Probes #1 and 2, respectively. The AFM height images are slope shaded.

calibration for this set of fused silica data. The effect of C_m uncertainties would be the largest for the biggest nanoindentations. For the biggest nanoindentations in this data set, an uncertainty of 10% in C_m resulted in uncertainties of less than 1 and 0.2% for A_0^{calc} and h_c, respectively. The effect was even smaller for the smaller nanoindentations. However, this uncertainty in C_m must be taken into consideration when correcting experimental P–h traces of other materials, especially for experiments with stiffer contact compliances.

After correcting the fused silica calibration P–h traces for C_m, C_p and h_c were calculated for each nanoindentation using the Oliver–Pharr method [5]. Figure 6a shows $J_0^{1/2} = C_p P_0^{1/2}$ plotted as a function of h_c. A threshold was observed at $h_c = 35$ nm. Above this threshold $J_0^{1/2}$ is constant and had an average value of 1.217 ± 0.002 μm/N$^{1/2}$ (uncertainty standard error). The $h_c = 35$ nm directly corresponded to the minimum SYS plot $P_0^{1/2} = 0.025$ N$^{1/2}$ threshold in Fig. 4a. The constant $J_0^{1/2}$ above the threshold size was a good check that the C_m was correct. The range of h_c over which $J_0^{1/2}$ was near the expected value of 1.22 μm/N$^{1/2}$ was also a useful indication of the range of nanoindentation sizes over which the probe exhibited the expected self-similar behavior of a Berkovich probe testing fused silica.

To calculate the probe area function, Eq. 6 was used to calculate A_0^{calc} for each nanoindent, and then Eq. 7 was fit to the A_0^{calc}–h_c data. After that, Eqs. 2 and 3 were used to calculate E_s, and Eq. 1 was used to calculate H. The $E_s = 72$ GPa in Fig. 6b was expected because that was the value assumed for A_0^{calc}. Checking that E_s was the constant 72 GPa over the

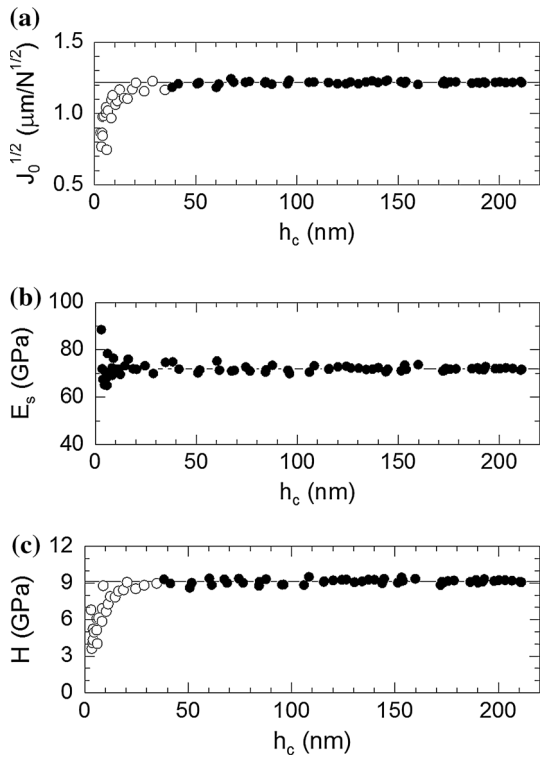

Figure 6 Values of **a** the square root of the Joslin-Oliver parameter ($J_0^{1/2}$), **b** elastic modulus (E_s), and **c** Meyer's hardness (H) for Berkovich Probe #1 as a function of contact depth (h_c). In **a** and **c**, the open symbols are the values below the threshold nanoindentation size ($h_c = 35$ nm) that are affected by tip imperfections or fused silica surface properties, and the solid symbols are the values above the threshold size. The solid line in **a** is the expected value of $J_0^{1/2} = 1.22$ μm/N$^{1/2}$ for Berkovich probe nanoindentations on fused silica [1, 14] and is included for comparison to the experimental $J_0^{1/2}$. The solid line in **b** is the assumed 72-GPa value for fused silica elastic modulus. The higher scatter of the E_s–h_c data for the smallest nanoindentations was likely caused by surface roughness or noise in the measured P and h that increased the uncertainty of the fits to the unloading segments when calculating the contact compliance. The solid line in **c** is 9.13 GPa, which is the average value of H above the threshold size ($h_c = 35$ nm).

entire range of nanoindentation sizes was useful only for confirming that the area function equation (Eq. 7) was fit well to the entire range of experimental A_0^{calc}–h_c data. It did not provide information about the accuracy of the C_m calculation, probe cleanliness, probe tip imperfections, or overall quality of the fused silica calibration nanoindentations. Because $H^{1/2} = J_0^{1/2}/E_{eff}$ and the probe area function was fit well over the entire range of experimental A_0^{calc}–h_c data, it was expected that the trend in H with nanoindentation size would be similar to the $J_0^{1/2}$–h_c plot. As expected, in Fig. 6c, a constant $H = 9.13 \pm 0.03$ GPa (uncertainty standard error) was observed only above the threshold nanoindentation size $h_c = 35$ nm (closed symbols in Fig. 6c). There was a general decrease in H with decreasing nanoindentation size below the threshold nanoindentation size (open symbols in Fig. 6c). The decrease for smaller nanoindentations may have been real and was likely the result of probe tip imperfections or fused silica surface properties.

To gain further insights into how the fused silica surface roughness may have affected the smallest nanoindents, an AFM height image was made of a residual nanoindentation impression near the threshold nanoindentation size (Fig. 7). The nanoindentation impression showed a triangular shape, similar to the shape of the probe contour plot (Fig. 5c) at a depth equal to h_c. However, the size of the nanoindentation was similar to the surface roughness features on the surface of the fused silica. So, although it is still uncertain whether the change in measured mechanical properties for the smallest nanoindentations for clean Probe #1 was caused by tip imperfections, fused silica surface properties, or an error in the assumption of constant E_s, Fig. 7 suggested that the surface roughness of the fused silica at least contributed to the observed scatter in E_s for the smallest nanoindentations [12]. Furthermore, the probe tip looked sharp in the AFM image at a depth of 20 nm and even below (Fig. 5a, c). It seems plausible that a fused silica standard with less surface roughness may have led to a more accurate calibration at shallower depths.

Discussion

Effects of $J_0^{1/2}$ and β on probe area function

The comparison of $J_0^{1/2}$ to the expected value of 1.22 μm/N$^{1/2}$ [1, 14] is one of the criteria used to decide whether or not fused silica calibration data are acceptable for C_m and probe area function calibrations. There are many factors that may cause $J_0^{1/2}$ to deviate from its expected value. As shown in this paper, $J_0^{1/2}$ can be affected by a dirty probe, probe tip imperfections, or fused silica surface properties. In addition, the $J_0^{1/2}$ value can also deviate from the expected 1.22 μm/N$^{1/2}$ value if the properties of the fused silica standard are different, the fused silica

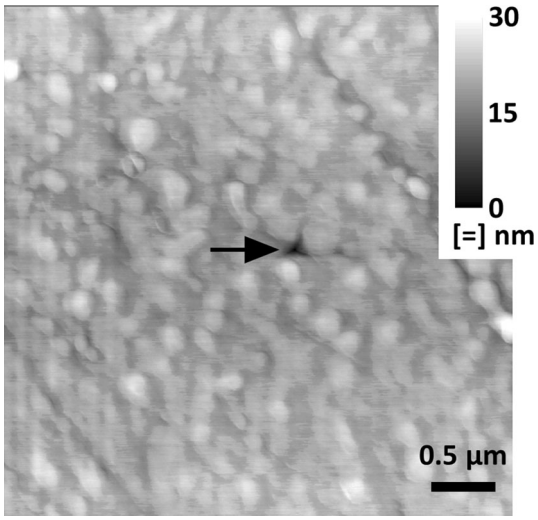

Figure 7 Atomic force microscopy (AFM) height image of a residual nanoindentation in fused silica. This nanoindentation was near the threshold nanoindentations size with $h_c = 36$ nm and $P_0^{1/2} = 0.023$ $N^{1/2}$. The nanoindentation is at the center of the image as indicated by the arrow. An edge fit background subtraction was performed to remove surface tilt.

surface is tilted, fracture events occur, or if there are errors in the C_m correction, Berkovich probe geometry, thermal drift correction, spring force calibration, applied load measurement, or probe displacement measurement. Because some experimental uncertainties are involved in all these factors that may affect $J_0^{1/2}$, this leads to the question of what an acceptable range for $J_0^{1/2}$ should be for fused silica calibration nanoindentations. Oliver and Pharr suggest, based on their experience, that for Berkovich nanoindentation on fused silica, the "proper" value of J_0 should be in the range of 0.015 ± 0.001 GPa^{-1} [1], which is equivalent to $J_0^{1/2} = 1.22 \pm 0.04$ $\mu m/N^{1/2}$. However, results within this range of acceptable values could lead to substantially different probe area functions. To directly quantify the effect of $J_0^{1/2}$ uncertainty on A_0^{calc}, Eq. 6 can be rewritten using $J_0^{1/2} = C_P P_0^{1/2}$ into the form

$$A_0^{calc} = \frac{1}{\beta^2}\frac{P_0}{\left(J_0^{1/2}\right)^2}\left[\frac{\pi^{1/2}}{2}\left(\frac{1-\nu_s^2}{E_s}+\frac{1-\nu_d^2}{E_d}\right)\right]^2 \quad (8)$$

In Eq. 8, A_0^{calc} depends on the squares of β and the experimental $J_0^{1/2}$. Those dependencies on a normalized A_0^{calc} are shown in Fig. 8. The Oliver and Pharr suggestion that a proper value of $J_0^{1/2}$ should be in the range of 1.22 ± 0.04 $\mu m/N^{1/2}$ can result in a difference in A_0^{calc} of $\pm$ 7%. This means that two "proper" calibrations of the same probe can result in probe area functions with a nearly 15% difference. From the author's experience, the $\pm$ 0.04 $\mu m/N^{1/2}$ uncertainty is much larger than it should be, and an uncertainty of $\pm$ 0.01 $\mu m/N^{1/2}$ is more appropriate. Although the acceptable range for $J_0^{1/2}$ is debatable, an acceptable solution would be for operators to report the fused silica calibration results.

Reporting, checking, and using Berkovich probe calibrations

Reporting Berkovich probe calibration results from fused silica nanoindentations will facilitate better comparisons between Berkovich probes both within and between research labs. In addition to the details of the procedure used for the calibration nanoindents, such as those listed in the Experimental Procedure section of this paper, the minimum reporting should address the following four elements:

1. The range of nanoindentation sizes over which the characteristic geometrically self-similar behavior of a Berkovich probe is observed in fused silica—This range includes the data that are not affected by probe tip imperfections, fused silica surface properties, or fracture events.
2. The reliability of the C_m calibration.

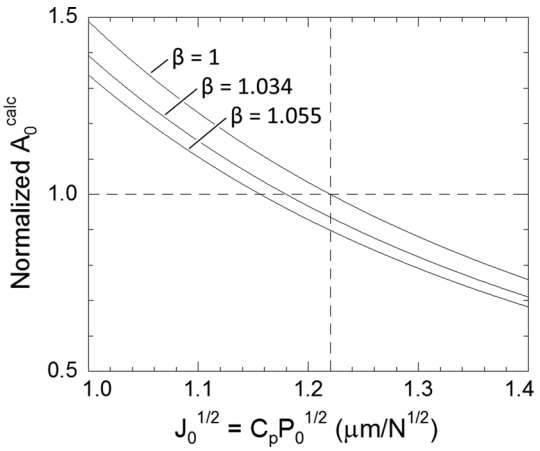

Figure 8 The normalized calculated area (A_0^{calc}) plotted as a function of the square root of the Joslin-Oliver parameter ($J_0^{1/2}$). The A_0^{calc} was calculated using Eq. 8 and was normalized to the value of A_0^{calc} at $J_0^{1/2} = 1.22$ $\mu m/N^{1/2}$ and $\beta = 1$. The β values of 1.034 and 1.055 were from King [24] and Strader et al. [19], respectively. The chosen value of β also had a large effect on the normalized A_0^{calc}. For example, the values of 1.034 and 1.055 resulted in a 7 and 11% decrease in normalized A_0^{calc} at $J_0^{1/2} = 1.22$ $\mu m/N^{1/2}$, respectively.

3. The accuracy of the probe area function equation fit to the A_0^{calc}–h_c data.
4. The quality of the instrument calibrations to measure loads and displacements.

All these elements can be addressed in a short statement. For example, this is achieved for clean Probe #1 with the statement: "Constant values of $J_0^{1/2} = 1.217 \pm 0.002$ μm/N$^{1/2}$, $E_s = 72.0 \pm 0.2$ GPa, and $H = 9.13 \pm 0.03$ GPa (uncertainties are standard errors) were assessed for fused silica calibration nanoindentations with h_c between 35 and 211 nm; no systematic variations of C_m or $J_0^{1/2}$ were observed in the systematic SYS plot analysis over this range of h_c." Element 1 is addressed by including the range of h_c over which a constant $J_0^{1/2}$, E_s, and H are observed and the statement that there is no systematic variation of $J_0^{1/2}$ in the systematic SYS plot analysis over the reported range of nanoindentation sizes. Element 2 is addressed by stating that $J_0^{1/2}$ is a constant value and there is no systematic variation of the C_m in the systematic SYS plot analysis. Element 3 is addressed by the statements that E_s and H were constants over the same range of nanoindentations as $J_0^{1/2}$, and that E_s is the assumed value of 72 GPa used in A_0^{calc} over the range of nanoindentation sizes. Element 4 is addressed by stating that the average constant value of $J_0^{1/2}$ is near the expected value of 1.22 μm/N$^{1/2}$. Including the uncertainties in the reporting sentence is useful for conveying the variation in the calibration data.

Another useful check for the calibration is comparing the fused silica H to the expected calculated H (H^{calc}) determined using the experimental $J_0^{1/2}$ and the equation

$$H^{calc} = \frac{P_0}{A_0^{calc}} = \beta^2 \left(J_0^{1/2}\right)^2 \left[\frac{\pi^{1/2}}{2}\left(\frac{1-\nu_s^2}{E_s} + \frac{1-\nu_d^2}{E_d}\right)\right]^{-2} \quad (9)$$

Similar to A_0^{calc} in Eq. 8, H^{calc} depends on the squares of β and the experimental $J_0^{1/2}$, and those dependences on H^{calc} are shown in Fig. 9. By inputting $J_0^{1/2} = 1.217$ μm/N$^{1/2}$ and $\beta = 1$ into Eq. 9, it was calculated that $H^{calc} = 9.14$ GPa for clean Probe #1 at h_c between 35 and 211 nm. This H^{calc} compared well to $H = 9.13 \pm 0.03$ GPa over this range. This check further verified that the calibration calculations were done correctly, such as the calculation of A_0^{calc} using Eq. 6. The chosen β has a substantial effect on fused silica H and must be taken into consideration when using H^{calc} to check the calibration data. The chosen β does not have an effect on fused silica E_s, because the effect of the β choice on A_0^{calc} is exactly compensated when the same value of β is used to calculate E_s using Eq. 3.

The lower end of the reported range of h_c over which constant $J_0^{1/2}$ values are measured (for example, $h_c = 35$ nm for clean Probe #1) could also be used as a metric of the size of the probe tip imperfections. However, this would require assuming that the dominate factor affecting the smallest nanoindentations is tip imperfections and not fused silica surface properties. For clean Probe #1, surface roughness may have been the dominating factor affecting the smallest nanoindentations (Fig. 7). Therefore, a fused silica surface with lowered roughness would be needed to more accurately characterize the sizes of probe tip imperfections. Nevertheless, by testing multiple probes in the same fused silica specimen, relative comparisons could be made, and recording this value of h_c would also be a useful way to track the size of the probe tip imperfections during the probe's lifetime.

If the probe area function is used in experiments for nanoindentations outside the reported range of h_c over which constant mechanical property values are assessed in fused silica, then the additional

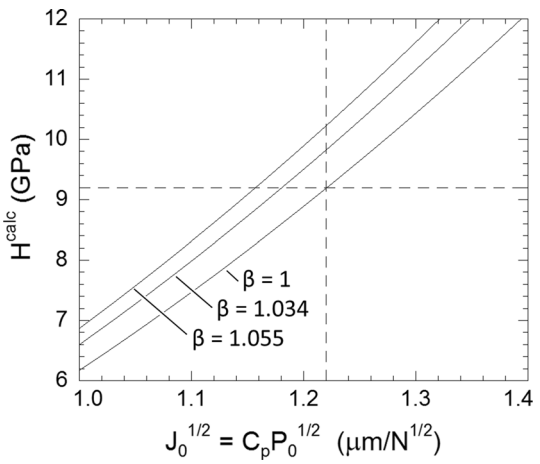

Figure 9 The calculated hardness (H^{calc}) plotted as a function of the square root of the Joslin-Oliver parameter ($J_0^{1/2}$) based on Eq. 9. The β values of 1.034 and 1.055 were from King [24] and Strader et al. [19], respectively. The chosen value of β also had a large effect on the H^{calc}. For example, the values of 1.034 and 1.055 resulted in a 7 and 11% increase in H^{calc} at $J_0^{1/2} = 1.22$ μm/N$^{1/2}$, respectively. Similar increases in experimental fused silica H would be expected if the corresponding values of β were used in the fused silica calibration analyses.

assumptions being employed in making such measurements must also be stated. For example, for larger nanoindents, the common assumptions are that the Berkovich probe effectively has an ideal geometry and that using the coefficient $c_0 = 24.5$ in fitting the probe area function (Eq. 7) accurately captures the shape. Assumptions for smaller nanoindentations are more problematic. One of the assumptions to calculate A_0^{calc} is that E_s is a constant 72 GPa. It is unknown how valid that assumption is for the smallest nanoindents, which are likely affected by the fused silica surface properties and probe tip imperfections. If constant E_s is assumed, then the calibration reporting should also include this information. Additionally, the full h_c range over which a constant E_s is calculated should be included to communicate the accuracy of the probe area function equation fit to the A_0^{calc}–h_c data that include the smaller nanoindentations. Furthermore, simulations using Berkovich probes modeled with spherical tip imperfections show that below a threshold nanoindentation size, H may be higher or lower than H that would have been assessed with an ideal Berkovich probe, and the trends depend on the tested material's ratio of yield stress to elastic modulus and strain hardening index [9, 12]. Therefore, caution must be exercised when using the probe area function to measure properties, especially H, in experimental materials near or below the lower range of h_c over which constant mechanical property values are assessed in fused silica.

Concluding remarks

The amount of user subjectivity in Berkovich probe C_m and probe area function calibrations can be decreased by using the demonstrated pre-nanoindentation liftoff and systematic SYS plot analyses. Additionally, because some user bias and uncertainties in calibration results will always exist, the fused silica calibration results should be reported to facilitate better comparisons of nanoindentation experiments performed with different Berkovich probes. Although any set of Berkovich probe fused silica calibration data could be analyzed using the SYS correlation and systematic SYS plot analysis as demonstrated in this paper, operators may also choose to utilize other area-independent correlations to assess the C_m [1, 6]. These other methods are similar to the SYS correlation method. To estimate C_m they rely on a straightline fit of calibration data chosen by the user that are assumed to exhibit size-independent mechanical properties. Therefore, the basic construct behind the systematic SYS plot analysis could be used to develop analogous systematic analyses of these other area-independent calibration methods.

Compliance with ethical standards

Conflict of interest The author declares that he has no conflict of interest.

References

[1] Oliver WC, Pharr GM (2004) Measurement of hardness and elastic modulus by instrumented indentation: advances in understanding and refinements to methodology. J Mater Res 19:3–20

[2] Fischer-Cripps AC (2006) Critical review of analysis and interpretation of nanoindentation test data. Surf Coat Technol 200:4153–4165

[3] Pethica JB, Hutchings R, Oliver WC (1983) Hardness measurement at penetration depths as small as 20 nm. Philos Mag A 48:593–606

[4] Doerner MF, Nix WD (1986) A method for interpreting the data from depth-sensing indentation instruments. J Mater Res 1:601–609

[5] Oliver WC, Pharr GM (1992) Improved technique for determining hardness and elastic modulus using load and displacement sensing indentation experiments. J Mater Res 7:1564–1580

[6] Fischer-Cripps AC (2004) Nanoindentation, 2nd edn. Springer, New York

[7] Stone DS, Yoder KB, Sproul WD (1991) Hardness and elastic modulus of TiN based on continuous indentation technique and new correlation. J Vac Sci Technol A 9:2543–2547

[8] Berkovich E (1951) Three-faceted diamond pyramid for micro-hardness testing. Ind Diam Rev 11:129–133

[9] Chen W, Li M, Zhang T, Cheng Y-T, Cheng C-M (2007) Influence of indenter tip roundness on hardness behavior in nanoindentation. Mater Sci Eng A 445–446:323–327

[10] Chen J, Bull SJ (2009) On the factors affecting the critical indenter penetration for measurement of coating hardness. Vacuum 83:911–920

[11] Fischer-Cripps AC (2010) The sharpness of a Berkovich indenter. J Mater Res 25:927–934

[12] Li M, Chen W, Cheng Y-T, Cheng C-M (2009) Influence of contact geometry on hardness behavior in nano-indentation. Vacuum 84:315–320

[13] Nix WD, Gao H (1998) Indentation size effects in crystalline materials: a law for strain gradient plasticity. J Mech Phys Solids 46:411–425

[14] Jakes JE, Frihart CR, Beecher JF, Moon RJ, Stone DS (2008) Experimental method to account for structural compliance in nanoindentation measurements. J Mater Res 23:1113–1127

[15] Jakes JE, Frihart CR, Beecher JF, Moon RJ, Resto PJ, Melgarejo ZH, Surez OM, Baumgart H, Elmustafa AA, Stone DS (2009) Nanoindentation near the edge. J Mater Res 24:1016–1031

[16] Jakes JE, Hunt CG, Yelle DJ, Lorenz LF, Hirth K, Gleber S-C, Vogt S, Grigsby W, Frihart CR (2015) Synchrotron-based x-ray fluorescence microscopy in conjunction with nanoindentation to study molecular-scale interactions of phenol-formaldehyde in wood cell walls. ACS Appl Mater Interfaces 7:6584–6589

[17] Bolshakov A, Pharr GM (1997) Inaccuracies in Sneddon's solution for elastic indentation by a rigid cone and their implications for nanoindentation data analysis. In: Gerberich WW, Gao H, Sundgren J-E, Baker SP (eds) Thin films: stresses and mechanical properties VI. Mater Res Soc Symp Proc 436, San Francisco, CA, USA, p 189

[18] Chudoba T, Jennett NM (2008) Higher accuracy analysis of instrumented indentation data obtained with pointed indenters. J Phys D Appl Phys 41:215407

[19] Strader JH, Shim S, Bei H, Oliver WC, Pharr GM (2006) An experimental evaluation of the constant β relating the contact stiffness to the contact area in nanoindentation. Philos Mag 86:5285–5298

[20] Joslin DL, Oliver WC (1990) New method for analyzing data from continuous depth-sensing microindentation tests. J Mater Res 5:123–126

[21] Sneddon IN (1965) Relation between load and penetration in axisymmetric Boussinesq problem for punch of arbitrary profile. Int J Eng Sci 3:47–57

[22] Pharr GM, Bolshakov A (2002) Understanding nanoindentation unloading curves. J Mater Res 17:2660–2671

[23] Harding DS, Oliver WC, Pharr GM (1994) Cracking during nanoindentation and its use in the measurement of fracture toughness. In: Demczyk BG, Williams ED, Garfunkel E, et al (eds) Evolution of thin-film and surface structure and morphology. Mater Res Soc Symp Proc 356, Pittsburgh, PA, p 663

[24] King RB (1987) Elastic analysis of some punch problems for a layered medium. Int J Solids Struct 23:1657–1664